Experimental observation of locally-resonant and Bragg band gaps for surface guided waves in a phononic crystal of pillars

Younes Achaoui
Institut FEMTO-ST, Université de Franche-Comté, CNRS, 32 Avenue de l'Observatoire, F-25044 Besançon, France

Abdelkrim Khelif
International Joint Laboratory Georgia Tech-CNRS, UMI 2958, 2-3 Rue Marconi, F-57070 Metz, France and Institut FEMTO-ST, Université de Franche-Comté, CNRS, 32 Avenue de l'Observatoire, F-25044 Besançon, France

Sarah Benchabane, Laurent Robert, and Vincent Laude
Institut FEMTO-ST, Université de Franche-Comté, CNRS, 32 Avenue de l'Observatoire, F-25044 Besançon, France
(Received 11 November 2010; published 14 March 2011)

We report on the experimental study of the propagation of surface guided waves in a periodic arrangement of pillars on a semi-infinite medium. Samples composed of nickel pillars grown on a lithium niobate substrate were prepared and wide bandwidth transducers were used for the electrical generation of surface elastic waves. We identify a complete band gap for surface guided waves appearing at frequencies markedly lower than the Bragg band gap. Using optical measurements of the surface vibrations and by comparison with a finite element model, we argue that the low frequency band gap arises because of local resonances in the pillars. When resonance is reached, the acoustic energy is confined inside the pillars and transmission through the array is strongly reduced. At higher frequencies and inside the Bragg band gap, the incident surface elastic waves are almost completely reflected and the observed exponential decay of the transmission is similar to the case of phononic crystals made of holes in a substrate.

DOI: 10.1103/PhysRevB.83.104201 PACS number(s): 43.20.+g, 43.35.+d, 63.20.Pw, 77.65.Dq

I. INTRODUCTION

The propagation of acoustic and elastic waves in periodic structures with spatially modulated elastic moduli and mass density has attracted significant interest during the last two decades, often in connection with the occurrence of frequency band gaps.[1,2] It has since then been observed that band gaps can arise because of two different mechanisms, Bragg interference and local resonances of substructures in the unit cell.[3–6] Bragg interference of waves scattered by inclusions occurs when the wavelength has a definite relation to the periodicity. In this case, it is customary to term the structure a phononic crystal. Bragg band gaps have been reported for waves in 2D and 3D phononic crystals including solid/fluid and solid/solid compositions.[7–9] Wave trapping, guiding, or even demultiplexing[10–12] through single and linear defects have also been reported. Local resonances of scatterers embedded inside a host matrix can also lead to the occurrence of frequency band gaps.[3] In this case, it is the normal resonance frequency of each individual in the unit cell, and not the lattice periodicity, that will condition the position of the gaps. These gaps can result from the Fano resonance of a localized state with a continuum of propagation modes:[4,13] At resonance, the energy of waves propagating in the matrix can be efficiently stored and delayed, while at antiresonance, wave propagation becomes prohibited. For a given periodicity, these locally resonant gaps can appear at frequencies markedly lower than the Bragg gap. This feature has been put forward to overcome the use of cumbersome devices while handling long-wavelength waves, e.g., in the sonic range.[3,4] The local resonance can indeed be tuned by using materials such as silicon rubber for which the sound velocity is two orders of magnitude lower than that of the host matrix. For such composites, polarization-dependent frequency band gaps were reported for bulk waves[14] and complete band gaps were reported for Lamb waves.[15] A local resonance can also be altered using shape design as in the case of Helmholtz resonators.[16]

Phononic crystals and locally resonant periodic structures can of course be made at very different scales. Still, the case of hypersonic elastic waves has recently drawn particular attention, in view of controlling the propagation of acoustic phonons at the micrometer scale, or even less.[17–19] For instance, Bragg band gaps for surface guided phonons in the case of arrays of holes in semi-infinite substrates have been predicted[20–23] and demonstrated experimentally.[24–26] In practice, the hole array defines a phononic crystal layer standing on a homogeneous semi-infinite substrate, rather than a genuine bidimensional phononic crystal: For frequencies above the Bragg band gap, the dispersion relation of surface phonons then lies within the sound cone[27] and a possible leakage into the bulk can result, although the quantitative analysis of this phenomenon is still an open problem. One possibility to overcome the radiation limit is to consider a free-standing thin membrane, or slab,[28] inside which energy is naturally confined. It has been shown that 2D phononic crystal slabs can exhibit omnidirectional Bragg band gaps in different compositions: steel beads or tungsten rods embedded in a membrane,[29,30] air holes etched in a slab,[31–35] or cylindrical rods added on the surface of the slab.[36–38] Another possibility that has been put forward in theory is to consider an array of pillars on a surface that introduces locally resonant band gaps at frequencies much lower than the Bragg band gap.[27] In this paper, we report on the experimental validation of this principle. We have specifically prepared phononic crystals constituted of an array of metal pillars on a piezoelectric

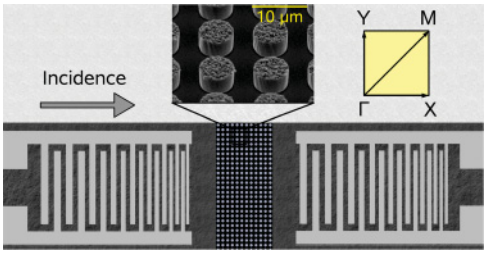

FIG. 1. (Color online) Schematic of the experimental setup used for investigating the propagation of surface phonons in a periodic array of pillars on a semi-infinite substrate. The nickel pillars shown as an inset have a radius of 3.2 μm and a height of 4.7 μm. They are arranged according to a square latttice with a pitch of 10 μm. Two chirped interdigital transducers generate and detect surface phonons thanks to the piezoelectric properties of the lithium niobate substrate. The phononic crystal has been studied in the three directions of highest symmetry of the Brillouin zone.

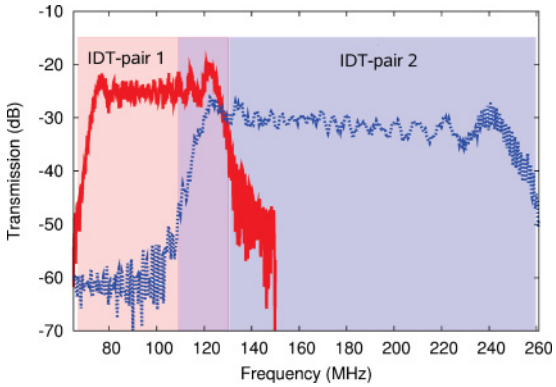

FIG. 2. (Color online) Measured electrical transmission T_{12} as a function of frequency for chirped interdigital transducers (IDTs) operating in a delay line configuration, without a phononic crystal in between the emitting and receiving IDTs. Two pairs of identical IDTs have been used in this study to cover a wide frequency bandwidth. They were designed to operate from 70 to 130 MHz and from 110 to 260 MHz, respectively.

substrate. Using wide-bandwidth interdigital transducers, we measure electrically the transmission of the samples. We further image the vibrations of the surface via heterodyne optical interferometry.[26] Combining these measurements, we identify the locally resonant and the Bragg band gap and highlight the differences between the two phenomena.

II. LOCALLY RESONANT BAND GAP

A typical phononic crystal sample used in this study is shown in Fig. 1. Fifteen rows of cylindrical nickel pillars arranged according to a 10-μm-pitch square lattice were grown on a Y + 128 lithium niobate substrate surface using electroplating. A thin film of copper was first deposited on the substrate to serve as a seed layer for the subsequent electroplating process. A resist mould allowing for the definition of the periodical array was then obtained by spin-coating and patterning of a thick photoresist layer. Nickel was later electrodeposited and the metal structures were eventually released by etching the resist away to form pillars with a 4.7 μm height and 3.2 μm radius. Lithium niobate was chosen as the substrate since this piezoelectric material allows for efficient generation and detection of surface acoustic waves (SAW) in a delay-line configuration. With a SAW velocity in the range of 3600 m/s, the Bragg band gap is expected at frequencies around 180 MHz.[22] Wide-bandwidth transduction of SAW was achieved using chirped interdigital transducers (IDTs) with a linear variation of the finger pitch. Figure 2 shows typical electrical transmission measurements obtained with a network analyzer for two different pairs of chirped IDTs in a delay-line configuration without the phononic crystal being present. The useful measurement bandwidth extends from 70 to 260 MHz. In the following, we define the electrical transmittance as the ratio of the transmission through the phononic crystal to the transmission without it.

Figure 3(a) displays the transmittance of the phononic crystal in the low frequency range extending from 70 to 105 MHz. The transmittance has been evaluated for the three main symmetry directions of the phononic crystal, referred to as the ΓX, ΓY, and ΓM directions of the first Brillouin zone. Note that waves propagating in the ΓX and the ΓY directions have different dispersions because of the material anisotropy of the substrate. A dip with an attenuation larger than 20 dB is observed at about 78 MHz for the three directions, suggesting the existence of a complete band gap for surface guided waves around this frequency.

Supplementary information about the interaction between the surface elastic waves and the pillars were obtained by imaging the out-of-plane motion of the surface at the frequency of the SAW using a heterodyne optical interferometer featuring a lateral resolution of about 800 nm. The obtained results are shown in Figs. 3(b) and 3(c). The monochromatic incident surface elastic wave was launched by one of the chirped IDTs. The optical scan was performed with a 2 μm step over an area size of 300 μm × 30 μm covering both the central part of the periodic array of pillars and free surface on its two sides. The data were afterward averaged along the Y-axis in order to get a cross section of the amplitude field. A frequency of 70 MHz, well below the band gap, was first selected. As Fig. 3(b) shows, surface waves are essentially transmitted at this frequency. Note that the resolution of the scan is comparable to the diameter of the pillars, which makes it difficult to resolve the vibration of the surface inside the periodic array. It can however be estimated that the amplitude of the vibration of the pillars at the exit of the structure does not essentially differ from the one measured at the entrance. At a frequency of 78 MHz, near the minimum of the electrical transmittance, the situation is quite different: The incident surface wave is efficiently reflected and a standing wave pattern originating from the interference of the incident and the reflected waves appears. Inside the periodic array, the amplitude of the vibration is dramatically enhanced at the first pillar, then decays exponentially toward the exit. A low transmission is observed at the exit side. Taking a closer look at the distribution of the vibration on the pillars, a characteristic spatial shape can be observed, with two peaks near the left and the right boundaries of the pillar and a central minimum. A higher resolution scan with a step of 0.3 μm was performed for one pillar of the second row, as

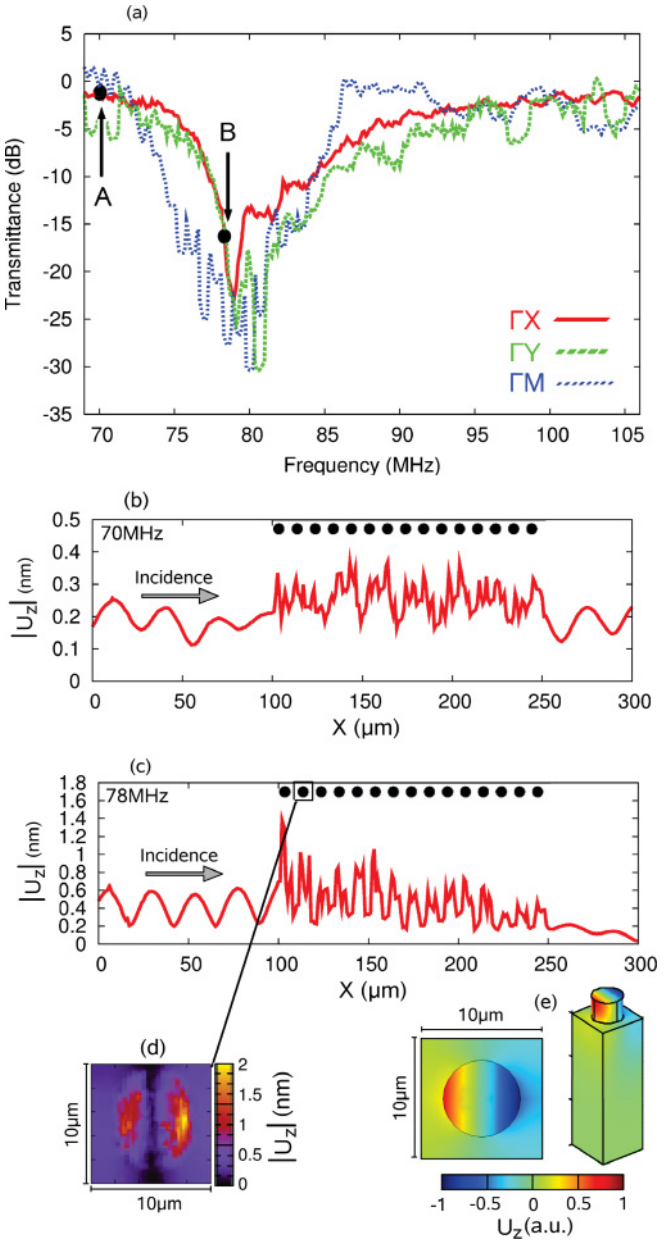

FIG. 3. (Color online) Investigation of surface phonon propagation in the frequency range around the locally resonant band gap. (a) Experimental transmittance of the periodic array of pillars for the three highest symmetry directions of the first Brillouin zone. The transmission dip around 78 MHz is the signature of a complete band gap for surface elastic waves. (b) The averaged cross section of the displacement of the surface, as measured using heterodyne optical interferometry for a frequency of 70 MHz (point A) and the ΓX propagation direction, shows essentially a transmission of the incident surface waves. (c) For a frequency of 78 MHz (point B), the same measurement shows the decaying storage of elastic energy along the pillar array. (d) An optical scan of a single pillar of the second row reveals the modal distribution of the surface displacement at the frequency of the transmission dip. (e) The finite element computation of the vertical displacement of the pillar confirms that the observed modal distribution is that of the first local resonance of the pillar.

shown in Fig. 3(d), confirming this observation. Figure 3(e) displays the computed modal shape of the first resonance of

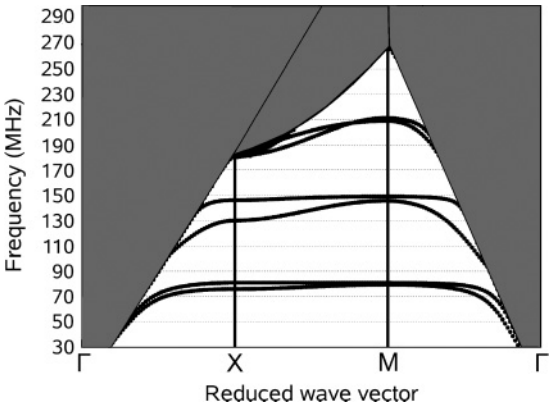

FIG. 4. Band structure of a periodic array of nickel pillars on a lithium niobate substrate computed using a finite element method[27] along the highest symmetry directions of the first Brillouin zone. The array is arranged according to a square lattice with a pitch $a = 10\ \mu$m. The radius of the pillar is $r = 3.2\ \mu$m and the height is $h = 4.7\ \mu$m. The gray region indicates the radiative region, or sound cone, of the substrate.

the pillar. The computation indicates that the resonant mode should be antisymmetrical along the direction of propagation and symmetrical along the orthogonal direction. As only the modulus of the vibration is measured, experiment and simulation are in excellent agreement. The full band gap around 78 MHz is therefore clearly linked to a local resonance of the pillars.

III. PHONONIC BAND STRUCTURE

The band structure for surface guided waves in a square array of nickel pillars sitting on a lithium niobate substrate was computed for the experimental geometrical parameters and is depicted in Fig. 4.The numerical computations were conducted using the finite element method described in Ref. 27 and take into account the anisotropy of the substrate. Some discrepancy between the theoretical and the experimental parameters may be present, due to the difficulty in controlling exactly the height and the rugosity of each pillar. The radiative region, or sound cone, has been indicated as the gray region. Its boundary is defined by the dispersion of the slowest bulk wave propagating in the substrate. Inside this region, true surface guided waves do not exist in principle, although leaky surface waves may still exist. The Rayleigh surface wave that is incident on the array of pillars in the experiments has a linear dispersion line outside the radiative region, although very close to its boundary. The dispersion of the modes of the considered phononic crystal can then be understood as resulting from the interaction of these waves guided by the surface with the pillars. Two band gaps for surface guided waves appear in the band structure. For frequencies well below the first band gap, the wave dispersion is close to that of the Rayleigh surface wave. In other words, the pillars do not significantly affect the propagation at long wavelengths. When the first resonance frequency of the pillars is reached, however, i.e., at about 80 MHz, the surface waves are strongly slowed down and exhibit a flat dispersion, which is a distinctive feature of efficient elastic energy storage.[39,40] For the geometrical parameters used here, the first band gap, of

the locally resonant type, appears at frequencies smaller by a factor of 2 than those of the second, Bragg band gap. It has been checked numerically that the position of the locally resonant gap is strongly affected by the pillar height. For instance, if this height equals the pitch of the array, the prohibited wavelength is around 200 μm, instead of about 50 μm in the present experiment. The position of the Bragg band gap, in contrast, remains quite stable. This dependence of the locally resonant band gap on the pillar height hence offers a practical means of controlling its frequency position. The third band has a rather linear dispersion, although its group velocity is significantly lower than that of the Rayleigh waves. In this case, the pillars have the role to slow the surface elastic wave. Let us here note that the fourth band is almost flat; it has been identified in the computations as the second resonant mode of the pillars, with an in-plane polarization.[27]

IV. BRAGG BAND GAP

Figure 5(a) displays the electrical transmittance of the phononic crystal in a frequency range extending from 100 to 230 MHz, for the ΓX direction. A wide Bragg band gap is observed for frequencies above 140 MHz. Below this frequency, the transmittance remains close to 1 and then drops abruptly at the band gap entrance. The band gap exit, however, is difficult to locate. It seems that a progressive retransmission occurs as the frequency increases from 180 MHz, culminating at 200 MHz, and falling again afterward. As predicted theoretically in Fig. 4, the radiative region is reached at about 180 MHz. Our computational model is unfortunately unable to predict the dispersion of the leaky surface guided waves in the radiative region, but we suggest that these may be responsible for the observed progressive retransmission.

Figure 5(b) shows an optical scan of the vibration of the surface at the frequency of 120 MHz, below the Bragg band gap, with experimental conditions identical to those of the optical scans presented in Fig. 3. The incident surface wave is partly reflected and partly transmitted by the phononic crystal of pillars. The amplitude of the surface vibration is higher inside the pillar array than on the free surface, in accordance with the observation that the pillars slow down the propagation of surface waves, resulting in the reduced group velocity of the third band in Fig. 4. The higher resolution scan performed for one pillar of the second row and shown in Fig. 5(c) indicates that the energy is mostly confined inside the pillar with a symmetric in-plane polarization. This observation is confirmed by the numerical simulation shown in Fig. 5(d).

Figure 5(e) shows the measured vibration of the surface at a frequency of 170 MHz, inside the Bragg band gap. An almost total reflection of the incident surface wave occurs, as can be evaluated from the standing wave pattern forming on the incident side of the phononic crystal. Inside the crystal itself, a strong exponential decay is observed. Such a decay is characteristic of Bragg destructive interferences and is reminiscent of similar observations for an array of holes in a substrate.[25,26]

V. CONCLUSION

In summary, we have studied experimentally how a periodic arrangement of pillars on a semi-infinite medium affects the

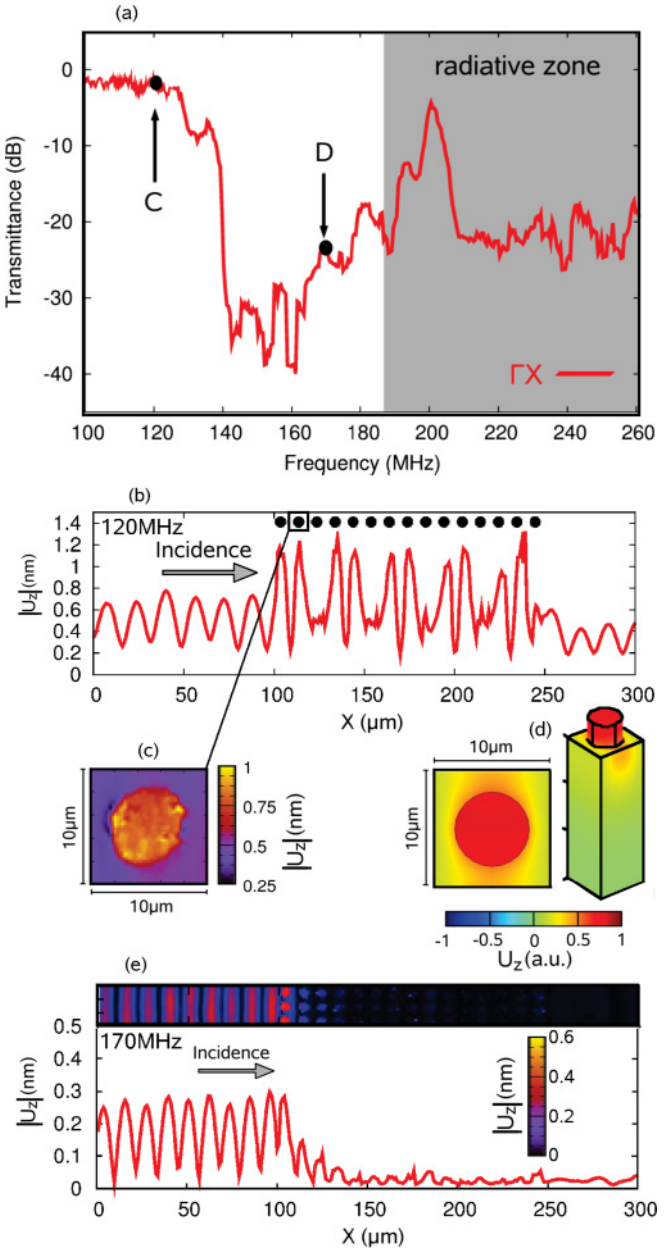

FIG. 5. (Color online) Investigation of surface phonon propagation in the frequency range around the Bragg band gap. (a) Experimental transmittance of the periodic array of pillars for the ΓX direction of the first Brillouin zone. A frequency band gap for surface elastic waves starts at 140 MHz. (b) The averaged cross section of the displacement of the surface, as measured using heterodyne optical interferometry for a frequency of 120 MHz (point C) and the ΓX propagation direction, shows a combination of transmission and reflection of the incident surface waves. (c) An optical scan of a single pillar of the second row reveals the modal distribution of the surface displacement at this frequency. (d) The finite element computation of the vertical displacement of the pillar is in agreement with the observed modal distribution of the pillar. (e) The averaged cross section of the displacement of the surface for a frequency of 170 MHz (point D) suggests that the incident surface waves are almost totally reflected and shows a strong exponential decay in the periodic array. The optical scan displayed as an inset illustrates how this reflection distributes spatially.

propagation of surface guided waves. For practical reasons, we have created samples composed of nickel pillars grown on a lithium niobate substrate. The very high piezoelectric coefficients of this material allowed us to use wide-bandwidth transducers for the electrical generation of surface elastic waves. In our experiments we have identified a complete band gap for surface guided waves appearing at frequencies markedly lower than the Bragg band gap. Using optical measurements of the surface vibrations and by comparison with a finite element model, we have found that the low frequency band gap arises because of a local resonance in the pillars. When resonance is reached, the acoustic energy is confined inside the pillars and the transmission through the pillar array is strongly reduced. At higher frequencies and inside the Bragg band gap, the incident surface elastic waves are almost completely reflected and the observed exponential decay of the transmission is similar to the case of phononic crystals made of holes in a substrate.

ACKNOWLEDGMENTS

The authors acknowledge fruitful discussion with J. Y. Rauch regarding technological issues during the preparation of the samples and the help of V. Petrini for wire bonding of the interdigital transducers. Financial support by the Agence Nationale de la Recherche under Grant No. ANR-09-BLAN-0167-01 is gratefully acknowledged.

[1] M. M. Sigalas and E. N. Economou, Solid State Commun. **86**, 141 (1993).
[2] M. S. Kushwaha, P. Halevi, L. Dobrzynski, and B. Djafari-Rouhani, Phys. Rev. Lett. **71**, 2022 (1993).
[3] Z. Liu, X. Zhang, Y. Mao, Y. Y. Zhu, Z. Yang, C. T. Chan, and P. Sheng, Science **289**, 1734 (2000).
[4] C. Goffaux, J. Sánchez-Dehesa, A. Levy Yeyati, P. Lambin, A. Khelif, J. O. Vasseur, and B. Djafari-Rouhani, Phys. Rev. Lett. **88**, 225502 (2002).
[5] T. Still, W. Cheng, M. Retsch, R. Sainidou, J. Wang, U. Jonas, N. Stefanou, and G. Fytas, Phys. Rev. Lett. **100**, 194301 (2008).
[6] X. Ao and C. T. Chan, Phys. Rev. B **80**, 235118 (2009).
[7] R. Martínez-Sala, J. Sancho, J. V. Sanchez, V. Gomez, J. Llinares, and F. Meseguer, Nature (London) **378**, 241 (1995).
[8] J. O. Vasseur, P. A. Deymier, B. Chenni, B. Djafari-Rouhani, L. Dobrzynski, and D. Prevost, Phys. Rev. Lett. **86**, 3012 (2001).
[9] A. Khelif, A. Choujaa, B. Djafari-Rouhani, M. Wilm, S. Ballandras, and V. Laude, Phys. Rev. B **68**, 214301 (2003).
[10] A. Khelif, A. Choujaa, S. Benchabane, B. Djafari-Rouhani, and V. Laude, Appl. Phys. Lett. **84**, 4400 (2004).
[11] A. Khelif, M. Wilm, V. Laude, S. Ballandras, and B. Djafari-Rouhani, Phys. Rev. E **69**, 067601 (2004).
[12] Y. Pennec, B. Djafari-Rouhani, J. O. Vasseur, H. Larabi, A. Khelif, A. Choujaa, S. Benchabane, and V. Laude, Appl. Phys. Lett. **87**, 261912 (2005).
[13] A. E. Miroshnichenko, S. Flach, and Y. S. Kivshar, Rev. Mod. Phys. **82**, 2257 (2010).
[14] G. Wang, X. Wen, J. Wen, L. Shao, and Y. Liu, Phys. Rev. Lett. **93**, 154302 (2004).
[15] J.-C. Hsu and T.-T. Wu, Appl. Phys. Lett. **90**, 201904 (2007).
[16] N. Fang, D. Xi, J. Xu, M. Ambati, W. Srituravanich, C. Sun, and X. Zhang, Nature Mater. **5**, 452 (2006).
[17] T. Gorishnyy, C. K. Ullal, M. Maldovan, G. Fytas, and E. L. Thomas, Phys. Rev. Lett. **94**, 115501 (2005).
[18] W. Cheng, J. Wang, U. Jonas, G. Fytas, and N. Stefanou, Nature Mater. **5**, 830 (2006).
[19] J.-F. Robillard, A. Devos, and I. Roch-Jeune, Phys. Rev. B **76**, 092301 (2007).
[20] Y. Tanaka and S. I. Tamura, Phys. Rev. B **58**, 7958 (1998).
[21] T.-T. Wu, Z.-G. Huang, and S. Lin, Phys. Rev. B **69**, 094301 (2004).
[22] V. Laude, M. Wilm, S. Benchabane, and A. Khelif, Phys. Rev. E **71**, 036607 (2005).
[23] J.-C. Hsu and T.-T. Wu, IEEE Trans. Ultrason. Ferroelectr. Freq. Control **53**, 1169 (2006).
[24] T.-T. Wu, L.-C. Wu, and Z.-G. Huang, J. Appl. Phys. **97**, 094916 (2005).
[25] S. Benchabane, A. Khelif, J.-Y. Rauch, L. Robert, and V. Laude, Phys. Rev. E **73**, 065601(R) (2006).
[26] K. Kokkonen, M. Kaivola, S. Benchabane, A. Khelif, and V. Laude, Appl. Phys. Lett. **91**, 083517 (2007).
[27] A. Khelif, Y. Achaoui, S. Benchabane, V. Laude, and B. Aoubiza, Phys. Rev. B **81**, 214303 (2010).
[28] A. Khelif, B. Aoubiza, S. Mohammadi, A. Adibi, and V. Laude, Phys. Rev. E **74**, 046610 (2006).
[29] F.-L. Hsiao, A. Khelif, H. Moubchir, A. Choujaa, C.-C. Chen, and V. Laude, Phys. Rev. E **76**, 056601 (2007).
[30] I. El-Kady, R. H. Olsson, and J. G. Fleming, Appl. Phys. Lett. **92**, 233504 (2008).
[31] S. Mohammadi, A. Eftekhar, A. Khelif, H. Moubchir, R. Westafer, W. Hunt, and A. Adibi, Electron. Lett. **43**, 898 (2007).
[32] B. Bonello, C. Charles, and F. Ganot, Appl. Phys. Lett. **90**, 021909 (2007).
[33] S. Mohammadi, A. Eftekhar, A. Khelif, W. Hunt, and A. Adibi, Appl. Phys. Lett. **92**, 221905 (2008).
[34] S. Mohammadi, A. Eftekhar, W. Hunt, and A. Adibi, Appl. Phys. Lett. **94**, 104301 (2009).
[35] M. F. Su, R. H. Olsson, Z. C. Leseman, and I. El-Kady, Appl. Phys. Lett. **96**, 053111(3) (2010).
[36] T.-T. Wu, Z.-G. Huang, T.-C. Tsai, and T.-C. Wu, Appl. Phys. Lett. **93**, 111902 (2008).
[37] Y. Pennec, B. Djafari-Rouhani, H. Larabi, J. O. Vasseur, and A. C. Hladky-Hennion, Phys. Rev. B **78**, 104105 (2008).
[38] T.-C. Wu, T.-T. Wu, and J.-C. Hsu, Phys. Rev. B **79**, 104306 (2009).
[39] V. Laude, L. Robert, W. Daniau, A. Khelif, and S. Ballandras, Appl. Phys. Lett. **89**, 083515 (2006).
[40] M. B. Dühring, V. Laude, and A. Khelif, J. Appl. Phys. **105**, 093504 (2009).